

# Biologically Inspired Coupled Beampattern Design\*

Murat Akçakaya, and Arye Nehorai\*  
 Electrical and Systems Engineering Department.  
 Washington University in St. Louis  
 St. Louis, Missouri 63130  
 Emails: makcak2, nehorai@ese.wustl.edu

**Abstract**—Inspired by the female *Ormia ochracea*'s mechanically coupled ears, we propose to design a small-size transmission coupled antenna array with high performance radiation pattern. The mechanical coupling provides the female *Ormia* with high localization accuracy despite the small distance between its ears compared with the incoming wavelength of the source signal. The mechanical coupling between the *Ormia*'s ears has been modeled by a pair of differential equations. In this paper, after solving these differential equations governing the *Ormia ochracea*'s ear response, we convert the response to the pre-specified radio frequencies. Using the converted response, we then design a biologically inspired uniform linear array composed of finite-length dipole antennas including also the undesired electromagnetic coupling due to the proximity of the elements. In our numerical examples, we compute the radiation intensity of the designed system for binomial and ordinary end-fire arrays to demonstrate the improvement in the half-power beamwidth, sidelobe suppression, and directivity of the radiation pattern due to the biologically inspired coupling.

## I. INTRODUCTION

The performance of an antenna array is directly proportional to the size of the array's electrical aperture, such that large aperture arrays are required to achieve highly directed, narrow beampatterns with low sidelobe levels [1]. However, for tactical and mobile applications, many civil and military sensing systems are confined to small spaces, requiring small-sized arrays, which hampers their radiation performance.

The concept of electrically small antenna arrays with high radiation performance, superdirective (supergain) arrays, is well known [1], and has attracted antenna researchers for the last few decades. Different methods have been proposed to achieve the superdirectivity by decoupling the antennas (reducing the effects of the undesired electromagnetic coupling among the antennas) and changing the current distributions applied to the array elements [2], [3], [4], [5].

In this paper, inspired by the coupled ears of a parasitoid tachinid fly called *Ormia ochracea*, we propose a beampattern design approach to achieve high performance with small aperture arrays. To perpetuate its species, a female *Ormia* must find a male field cricket using the cricket's mating call. The female *Ormia* has a remarkable ability to locate these crickets very accurately using binaural (two-ear) cues (interaural differences in intensity and arrival time from an incident acoustic wave).

This is unexpected due to the significant mismatch between the wavelength of the cricket's call (about 7 cm) and the distance between the fly's ears (about 1.2 mm) which gives rise to cues that are extremely small to be detectable by the central nervous system of the fly [6]- [11].

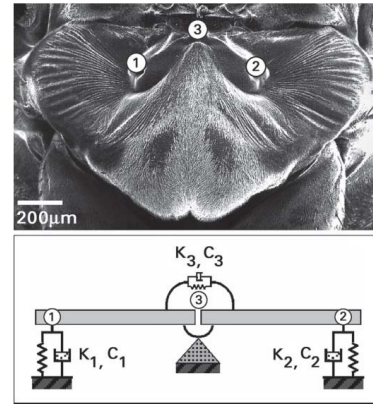


Fig. 1. Mechanical model of the female *Ormia ochracea*'s ears [12].

Experimental research in [12] explains that the *Ormia*'s localization ability arises from a mechanical coupling between its ears, modeled as a system consisting of spring and dash-pots (with six key parameters:  $\{(c_i, k_i) : i = 1, 2, 3\}$ ) as shown in Fig. 1. In the equivalent mechanical system, the intertympanal bridge (the cuticular connecting structure) is assumed to consist of two rigid bars connected at the pivot through a coupling spring  $k_3$  and dash-pot  $c_3$ . The springs and dash-pots located at the extreme ends of the bridge approximate the dynamical properties of the tympanic membranes, sensory organs, and surrounding structures in the *Ormia*'s two ears.

In our previous work [13], we analyzed the localization accuracy of the *Ormia*'s coupled ears using a statistical approach, namely by computing the Cramér-Rao bound (CRB) [14]. We showed quantitatively that the coupling improves the accuracy of direction of arrival (DOA) estimation in the presence of interference and noise.

In Section II of this paper, we introduce the array-factor design for a uniform linear array inspired by the coupled ears of *Ormia*. First, we obtain the *Ormia*'s coupled ears' response by solving the second order differential equations. Then we convert this response to fit the desired radio frequencies. Together with the undesired electromagnetic coupling among

\* This work was supported by DARPA Grant No. HR0011-09-P-0007, the Department of Defense under Air Force Office of Scientific Research MURI Grant FA9550-05-1-0443 and ONR Grant N000140810849.

\* Corresponding author.

the array elements (due to their proximity), we include the biologically inspired coupling (BIC) in the array factor. In Section III, we assume finite-length dipoles as the antenna elements and compute the radiation intensity, and accordingly the directivity gain, half-power beamwidth (HPBW) and side lobe level (SLL) as radiation performance measures. In Section IV, we compare the radiation performances of the biologically inspired coupled and standard antenna arrays, demonstrating the improvement due to the BIC. By standard antenna array we refer to a system without BIC. Finally we provide concluding remarks in Section V.

## II. ARRAY FACTOR

In this section, we compute the array factor of the proposed biologically inspired uniform linear array (ULA). We start with the array factor of a standard ULA, positioned without loss of generality along the  $z$ -axis (see Fig. 2). Since we focus on systems confined in small spaces, we also consider the undesired electromagnetic coupling between the array elements.

Under the far-field radiation and narrow-band signal assumption, we modify the uniform linear array factor to include the undesired coupling between the elements (see also [15]):

$$\text{AF}(\theta) = \sum_{m=1}^M p_m \exp(-j(m-1)(\omega\Delta + \beta)), \quad (1)$$

where,

- $\text{AF}(\theta)$  is the radiation pattern (desired amplitude and phase in each direction) of  $M$ -element array assuming isotropic antennas, which depends on the positions and excitations of the sensing elements in the system;
- $\mathbf{p} = [p_1, \dots, p_M]^T = \mathbf{C}\mathbf{v}_g$  is the vector of the currents on the antennas;
- $\mathbf{v}_g = [v_1, \dots, v_M]^T$  is the vector of generator (excitation) voltages at the input of the antennas,
- $\mathbf{C}$  is the undesired electromagnetic coupling between the array elements, (a transformation matrix, transforming generator voltages to the induced currents on each antenna);
- $\omega = 2\pi f$  with  $f$  as the frequency of the radiated signal;
- $\Delta = \frac{d \sin \theta}{v}$  is the interelement time difference;
- $d$  is the interelement distance;
- $v$  is the speed of signal propagation in the medium;
- $\theta$  is the elevation angle (see Fig. 2); and
- $\beta$  is the excitation phase.

We compute  $\mathbf{C}$  similar to [15] as a function of self and mutual impedances between the antennas (see also discussions in [16] and [17]). When the mutual impedances are zero, when there is no electromagnetic coupling,  $\mathbf{C}$  reduces to a diagonal matrix. We compute the self and mutual impedances, assuming finite-length dipole antennas as the elements of the array, as explained in [1, Chapter 8], see also Section IV. Note that the standard literature often ignores  $\mathbf{C}$ , which is reasonable for sufficiently large inter-elemental distances.

The usual goal of the array-factor design is to select the excitation voltages,  $\mathbf{v}_g$ , and phase,  $\beta$ , to obtain a desired radiation pattern. Our goal is to include the BIC in the

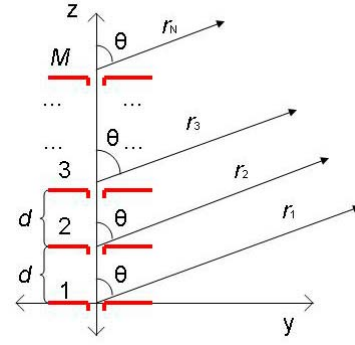


Fig. 2. Far-field radiation geometry of  $M$ -element antenna array.

array factor for fixed  $\mathbf{v}_g$  and  $\beta$  values and demonstrate the improvement in the directivity gain, HPBW and SLL of the radiation pattern.

In the following we modify (1) to include also the BIC. We obtain the response of the Ormia's coupled ears, and convert this response to fit the desired radio frequencies. Then using the converted response, we design a biologically inspired array factor.

### A. Response of the Ormia's Coupled Ears

To obtain the response of the Ormia's coupled ears, we solve the second-order differential equations governing the mechanical model proposed in [12] for the Ormia's ears (Fig. 1), and find the corresponding transfer function. The governing differential equations are:

$$\begin{bmatrix} x_1(t, \Delta) \\ x_2(t, \Delta) \end{bmatrix} = \begin{bmatrix} k'_1 & k_3 \\ k_3 & k'_2 \end{bmatrix} \begin{bmatrix} y_1 \\ y_2 \end{bmatrix} + \begin{bmatrix} c'_1 & c_3 \\ c_3 & c'_2 \end{bmatrix} \begin{bmatrix} \dot{y}_1 \\ \dot{y}_2 \end{bmatrix} + \begin{bmatrix} m_0 & \\ & m_0 \end{bmatrix} \begin{bmatrix} \ddot{y}_1 \\ \ddot{y}_2 \end{bmatrix} \quad (2)$$

where

- $x_i(t, \Delta)$ ,  $i = 1, 2$ , are the input signals;
- $y_i(t)$ ,  $i = 1, 2$ , are the displacements of each ear;
- $k'_i = k_i + k_3$ , and  $c'_i = c_i + c_3$ ,  $i = 1, 2$ ; and
- $m_0$ ,  $k$ 's, and  $c$ 's are the effective mass, spring and dashpot constants, respectively.

To solve the differential equations, we apply the Laplace transform to (2) assuming zero initial values,

$$\begin{bmatrix} Y_1(s) \\ Y_2(s) \end{bmatrix} = 1/P(s) \begin{bmatrix} D_2(s) & -N(s) \\ -N(s) & D_1(s) \end{bmatrix} \begin{bmatrix} X_1(s) \\ X_2(s) \end{bmatrix}, \quad (3)$$

where

- $Y_1(s)$  and  $Y_2(s)$  are the Laplace transforms of  $y_1(t)$  and  $y_2(t)$ ,
- $X_1(s)$  and  $X_2(s)$  are the Laplace transforms of  $x_1(t)$  and  $x_2(t)$ ,
- $D_1(s) = m_0 s^2 + (c_1 + c_3)s + k_1 + k_3$  and  $D_2(s) = m_0 s^2 + (c_2 + c_3)s + k_2 + k_3$ ,
- $N(s) = c_3 s + k_3$  (coupling effect),
- $P(s) = D_1(s)D_2(s) - N^2(s)$  is the characteristic function.

We obtain the Laplace transform of the impulse responses associated with (2) by substituting

$$\begin{aligned} x_1(t) &= \delta(t) \rightarrow x_1(s) = 1, \\ x_2(t) &= x_1(t - \Delta) \rightarrow x_2(s) = e^{-s\Delta}. \end{aligned}$$

Then the system responses are

$$\begin{aligned} H_1(s, \Delta) &= (D_2(s) - N(s)e^{-s\Delta})/P(s), \\ H_2(s, \Delta) &= (D_1(s)e^{-s\Delta} - N(s))/P(s). \end{aligned} \quad (4)$$

Substituting  $s = j\omega$ , we compute the frequency responses of the Ormia's coupled ears. Using these responses, in [13], we demonstrated that the coupling amplifies the amplitude and phase differences between the responses of the Ormia's two ears.

Note that these equations represent a two-input two-output filter system.

### B. Converting to Desired Radio Frequencies for Array Response Design

We now modify the frequency response of the Ormia's ears to fit the desired radio frequencies by re-computing the poles of the transfer function in (3), the roots of  $P(s) = D_1(s)D_2(s) - N^2(s) = 0$ . We shift the resonance frequencies of the system by changing the imaginary parts of the poles. This corresponds to changing the system parameters, namely mass, spring and dash-pot constants defined in the analogous mechanical model (see (2)). We scale the resonant frequency locations (controlling the imaginary parts of the poles) and the real parts of the poles using different constants. Therefore, we keep the real parts as free parameters. In a journal version of this manuscript, we optimize the coupling using the real parts of the poles without modifying the resonant frequencies [18].

We obtain the ratio between the frequency responses

$$\frac{H_2(\omega, \Delta)}{H_1(\omega, \Delta)} = \frac{D_1(j\omega)e^{-j\omega\Delta} - N(j\omega)}{D_2(j\omega) - N(j\omega)e^{-j\omega\Delta}}. \quad (5)$$

choosing the frequency  $\omega$  depending on the application (see also Section IV).

### C. Biologically Inspired Coupled Array Factor

To apply the BIC concept to the array factor in (1), we replace the exponential terms in (1) with the ratio in (5)

$$AF_I(\theta) = \sum_{m=1}^M p_m \left( \frac{H_2(\omega, \Delta, \beta)}{H_1(\omega, \Delta, \beta)} \right)^{(m-1)}, \quad (6)$$

where

$$\frac{H_2(\omega, \Delta, \beta)}{H_1(\omega, \Delta, \beta)} = \frac{D(j\omega) \exp(-j(\omega\Delta + \beta)) - N(j\omega)}{D(j\omega) - N(j\omega) \exp(-j(\omega\Delta + \beta))},$$

with  $D(j\omega)$  and  $N(j\omega)$  as defined after (3), substituting  $s = j\omega$ . We assume identical antennas  $D_1(j\omega) = D_2(j\omega) = D(j\omega)$ . The ratio in (5) generalizes the exponential terms in (1) to include the BIC.

Note that  $N(j\omega)$  represents the BIC and when there is no coupling ( $N(j\omega) = 0$ ),  $AF_I(\theta)$  in (6) reduces to  $AF(\theta)$  in (1). In this paper, we analytically demonstrate the biologically inspired beampattern design. The actual implementation is left for a future work.

## III. RADIATION INTENSITY, DIRECTIVITY, HALF-POWER BEAMWIDTH AND SIDE LOBE LEVEL

In this section, we describe our measures to analyze the radiation performance. First, taking into account the antenna factor (element factor) and the BIC, we compute the radiation intensity of the antenna array in a given direction [1]

$$U_I(\theta, \phi) = [EF(\theta, \phi)]_n^2 [AF_I(\theta)]_n^2, \quad (7)$$

where

- $[EF(\theta, \phi)]_n$  is the normalized element factor, far-zone electric field of a single element (in our work we assume that the array is formed with finite-length dipoles, see also Section IV),
- $[AF_I(\theta)]_n$  is the normalized array factor,
- $U_I(\theta, \phi)$ , the radiation intensity in a given direction, is the power radiated from an antenna array per unit solid angle.
- Hence the radiated power  $P_{\text{rad}}$  is

$$P_{\text{rad}} = \int_0^{2\pi} \int_0^\pi U_I(\theta, \phi) \sin \theta \, d\theta \, d\phi,$$

where  $\theta$  and  $\phi$  are the elevation and azimuth angles, respectively,  $\sin \theta \, d\theta \, d\phi$  is the unit solid angle.

Using the radiation intensity, we consider the following measures to analyze the performance of the beampattern design:

- The directivity,  $D_I(\theta, \phi)$ , is the ratio of the radiation intensity in a given direction to the average radiation intensity.

$$D_I(\theta, \phi) = \frac{4\pi U_I(\theta, \phi)}{P_{\text{rad}}}, \quad (8)$$

where  $\frac{1}{4\pi} P_{\text{rad}}$  is the average radiation intensity over all angles. In our work, for comparison purposes, we consider the directivity gain in a desired direction (at elevation  $\theta = 0^\circ$  and azimuth  $\phi = 90^\circ$ , see also Section IV).

- Half-power beamwidth, HPBW, in terms of the elevation angle,  $\theta$ , for a fixed azimuth angle,  $\phi$ . HPBW is defined as the angle between two half power directions [1].
- Sidelobe level (SLL) defined as the maximum value of the radiation pattern in any direction other than the desired one (direction other than  $\theta = 0^\circ$  on  $\phi = 90^\circ$  plane for our case).

The directivity gain, HPBW and SLL measure how effectively the power is directed (steered) in a given direction. For a good performance, it is desirable to have large  $D_I(\theta, \phi)$ , small SLL and narrow HPBW in a desired direction.

## IV. NUMERICAL EXAMPLES

In this section, we compare the radiation performances of the biologically inspired coupled and standard antenna arrays. We plot the radiation pattern and compare the directivity gain, half-power beamwidths and sidelobe attenuation of these systems using the following scenario. In the following discussion by BIC array we refer to an antenna array with BIC.

|                | Uniform           |                  | Binomial          |                  |
|----------------|-------------------|------------------|-------------------|------------------|
|                | $d = 0.25\lambda$ | $d = 0.1\lambda$ | $d = 0.25\lambda$ | $d = 0.1\lambda$ |
| BIC Array      | 19.22             | 16.92            | 16.86             | 15.19            |
| Standard Array | 13.96             | 10.77            | 10.81             | 8.08             |

TABLE I  
DIRECTIVITY GAINS OF THE ANTENNA ARRAYS IN THE DESIRED  
DIRECTION  $\theta = 0^\circ$  AND  $\phi = 90^\circ$  (dB)

|                | Uniform           |                  | Binomial          |                  |
|----------------|-------------------|------------------|-------------------|------------------|
|                | $d = 0.25\lambda$ | $d = 0.1\lambda$ | $d = 0.25\lambda$ | $d = 0.1\lambda$ |
| BIC Array      | $19^\circ$        | $28^\circ$       | $24^\circ$        | $30^\circ$       |
| Standard Array | $45^\circ$        | $62^\circ$       | $63^\circ$        | $76^\circ$       |

TABLE II  
HALF-POWER BEAMWIDTHS OF THE ANTENNA ARRAYS (DEGREES)

- We consider uniform (uniform excitation voltages) ordinary and binomial (binomial expansion coefficients as the excitation voltage values) end-fire arrays [1, Chapter 8], maximum at  $\theta = 0^\circ$ , then  $\beta = -w\Delta$ .
- Frequency of interest,  $f = 1$  GHz.
- Uniform linear array composed of 20 identical dipole antennas.
- The undesired coupling matrices,  $C$  for  $0.5\lambda$ -wavelength antenna system with different interelement distances ( $d = 0.25\lambda$  and  $d = 0.1\lambda$ ) are calculated according to [1, Chapter 8] for finite-length thin-dipole antennas.
- The antennas are located on the  $z$ -axis parallel to  $y$ -axis, then assuming azimuth  $\phi = 90$  (on the  $y$ - $z$  plane, see Fig. 2), the element factor for a finite-length dipole antenna is computed as

$$EF(\theta, 90^\circ) = \left[ \frac{\cos\left(\frac{kl}{2} \sin \theta\right) - \cos\left(\frac{kl}{2}\right)}{\cos \theta} \right].$$

where  $k = \frac{2\pi}{\lambda}$ ,  $\lambda$  is the wavelength of the radiated signal and  $l$  is the length of each antenna.

Recall that we focus on 2-D beampattern design in terms of elevation angle,  $\theta$ .

We demonstrate our results in Figs 3 and 4, and summarize the calculated directivity gains, and HPBW values in Tables I and II, respectively. We observe that the BIC array with uniform excitation voltages outperforms the uniform standard array in terms of sidelobe suppression, directivity, and HPBW (see Fig. 3, and Tables I and II). For binomial array, in Fig. 4, we observe that neither the standard nor the BIC arrays have sidelobes, but the BIC array has much narrower HPBW and hence better directivity gain (see also Tables I and II). The physical reason of the improvement in the radiation performance is the BIC that works as a multi-input multi-output filter, magnifying the amplitude and phase differences (time differences) between the outputs of the successive antennas and creating a virtual array with a larger aperture. In the beampattern design, the virtual array with larger aperture creates a radiation pattern with higher directivity and sidelobe suppression, and lower half-power beamwidth. Note that in these examples the effect of the BIC increases as the distance between the antennas,  $d$ , decreases.

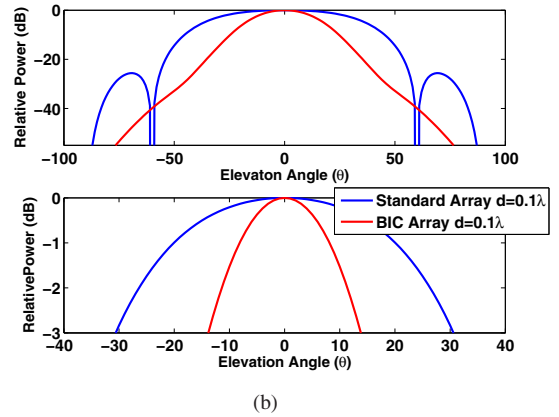
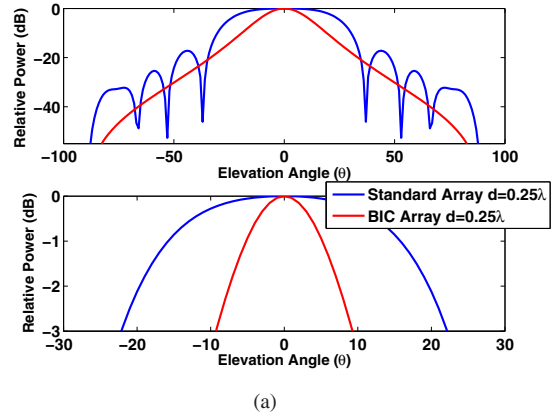


Fig. 3. Power pattern of the uniform standard and BIC ordinary end-fire antenna arrays for (a)  $d = 0.25\lambda$ , (b)  $d = 0.1\lambda$  interelement spacings. Bottom halves of the figures present the half-power beamwidth.

## V. CONCLUSION

We designed a coupled antenna system inspired by the mechanically coupled ears of the *Ormia ochracea*. After computing the response of the mechanical model representing the coupling between the *Ormia*'s ears, we converted it to the desired radio frequencies. Then we designed the biologically inspired coupled antenna array by generalizing the array response of a uniform linear antenna array to include the converted response (coupling the antennas using the biologically inspired coupling). Since we focus on systems confined to small spaces, we also considered the undesired electromagnetic coupling among the array elements. We computed the radiation intensity, and accordingly the directivity gain, the half-power beamwidth and the sidelobe level of the biologically inspired and standard antenna arrays as the performance measures. We demonstrated the improvement in the radiation performance due to the biologically inspired coupling. In our future work, we will focus on the implementation of the beampattern design, 3-D beampattern design, and non-linear antenna arrays (circular, etc.).

## REFERENCES

- [1] C. Balanis, *Antenna Theory: Analysis and Design*. New York: John Wiley and sons, Inc., 1982.

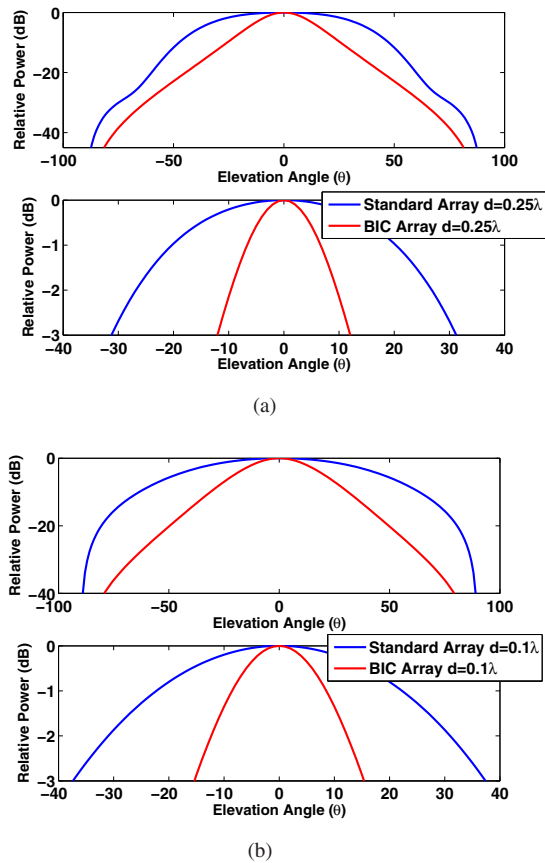


Fig. 4. Power patterns of the binomial standard and BIC end-fire antenna arrays for (a)  $d = 0.25\lambda$ , (b)  $d = 0.1\lambda$  interelement spacings. Bottom halves of the figures present the half-power beamwidth.

- [2] D. Tucker, "Superdirective arrays: the use of decoupling between elements to ease design and increase bandwidth," *Radio and Electronic Engineer*, vol. 34, no. 4, pp. 251–256, October 1967.
- [3] E. Newman, J. Richmond, and C. Walter, "Superdirective receiving arrays," *IEEE Trans. Antennas Propag.*, vol. 26, no. 5, pp. 629–635, Sep 1978.
- [4] B. Popovic, B. Notaros, and Z. Popovic, "Supergain antennas: a novel philosophy of synthesis and design," in *Proc. 26th URSI General Assembly*, Toronto, Ontario, Canada, August 1999, p. 7675.
- [5] T. Lee and Y. E. Wang, "Mode-Based Information Channels in Closely Coupled Dipole Pairs," *IEEE Trans. Antennas Propag.*, vol. 56, pp. 3804–3811, Dec. 2008.
- [6] W. Cade, "Acoustically Orienting Parasitoids: Fly Phonotaxis to Cricket Song," *Science*, vol. 190, pp. 1312–1313, Dec. 1975.
- [7] D. Robert, M. J. Amoroso, and R. R. Hoy, "The evolutionary convergence of hearing in a parasitoid fly and its cricket host," *Science*, vol. 258, no. 5085, pp. 1135–1137, 1992.
- [8] D. Robert, M. P. Read, and R. R. Hoy, "The tympanal hearing organ of the parasitoid fly *Ormia ochracea* (diptera, tachinidae, ormiini)," *Cell Tissue Res.*, vol. 275, no. 1, pp. 63–78, 1994.
- [9] D. Robert, R. N. Miles, and R. R. Hoy, "Directional hearing by mechanical coupling in the parasitoid fly *Ormia ochracea*," *J. Comp. Physiol. A*, vol. 179, no. 1, pp. 29–44, Jul. 1996.
- [10] —, "Tympanal mechanics in the parasitoid fly *Ormia ochracea*: intertympanal coupling during mechanical vibration," *J. Comp. Physiol. A*, vol. 183, no. 4, pp. 443–452, Oct. 1998.
- [11] A. C. Mason, M. L. Oshinsky, and R. R. Hoy, "Hyperacute directional hearing in a microscale auditory system," *Nature*, vol. 410, pp. 686–690, Apr. 2001.
- [12] R. N. Miles, D. Robert, and R. R. Hoy, "Mechanically coupled ears for directional hearing in the parasitoid fly *Ormia ochracea*," *J. Acoust. Soc. Am.*, vol. 98, no. 6, pp. 3059–3070, 1995.
- [13] M. Akcakaya and A. Nehorai, "Performance analysis of *Ormia*

*ochracea*'s coupled ears," *J. Acoust. Soc. Am.*, vol. 124, no. 4, pp. 2100–2105, Oct. 2008.

- [14] S. Kay, *Fundamentals of statistical signal processing: estimation theory*. Upper Saddle River, NJ: Prentice Hall PTR, 1993.
- [15] J. Allen and B. Diamond, "Mutual coupling in array antennas," MIT Lincoln Laboratory, Lexington, MA, Tech. Rep. 424, Oct. 1966.
- [16] I. Gupta and A. Ksienski, "Effect of mutual coupling on the performance of adaptive arrays," *IEEE Trans. Antennas Propag.*, vol. 31, no. 5, pp. 785–791, Sep 1983.
- [17] T. Svantesson, "The effects of mutual coupling using a linear array of thin dipoles of finite length," in *Proc. Ninth IEEE SP Workshop on Statistical Signal and Array Proces.*, Sep 1998, pp. 232–235.
- [18] M. Akcakaya and A. Nehorai, "Biologically inspired coupled antenna beam pattern design," submitted for publication to *Bioinspiration and Biomimetics*.